Structural Characterization of Proteins with an Attached ATCUN Motif by Paramagnetic Relaxation Enhancement NMR Spectroscopy

Logan W. Donaldson,[†,#] Nikolai R. Skrynnikov,*[,†] Wing-Yiu Choy,[†,||] D. Ranjith Muhandiram,[†] Bibudhendra Sarkar,[||,‡,⊥] Julie D. Forman-Kay,[||,‡] and Lewis E. Kay*[,†,‡,§,⊥]

Contribution from the Department of Medical Genetics, Department of Biochemistry, Department of Chemistry, University of Toronto, Toronto, ON, Canada, M5S 1A8, Structural Biology and Biochemistry Program, Hospital for Sick Children, Toronto, ON, Canada, M5G 1X8, Department of Biology, York University, Toronto, ON, Canada, M3J 1P3, and Protein Engineering Network Centres of Excellence

Received May 21, 2001. Revised Manuscript Received July 16, 2001

Abstract: The use of a short, three-residue Cu^{2+}-binding sequence, the ATCUN motif, is presented as an approach for extracting long-range distance restraints from relaxation enhancement NMR spectroscopy. The ATCUN motif is prepended to the N-termini of proteins and binds Cu^{2+} with a very high affinity. Relaxation rates of amide protons in ATCUN-tagged protein in the presence and absence of Cu^{2+} can be converted into distance restraints and used for structure refinement by using a new routine, PMAG, that has been written for the structure calculation program CNS. The utility of the approach is demonstrated with an application to ATCUN-tagged ubiquitin. Excellent agreement between measured relaxation rates and those calculated on the basis of the X-ray structure of the protein have been obtained.

Introduction

Paramagnetic probes have been utilized to obtain valuable information about the structure of biomolecules in many recent NMR studies. A growing number of applications involve measurements of nuclear spin relaxation enhancements,[1] including autorelaxation of two-spin order[2a] and dipole−dipole (dipole-Curie-spin) cross-correlated relaxation,[2b,c] as well as measurements of pseudocontact[3a,b] and contact[3c] shifts. In addition, paramagnetic substances have been used in biomolecular NMR as intermolecular relaxation agents[4] and magnetic alignment agents facilitating the measurements of residual dipolar couplings.[5] Paramagnetic structural restraints are particularly useful when conventional NOEs are unavailable or difficult to interpret because of complex molecular dynamics, such as at protein−protein or protein−nucleic acid interfaces[6] and in unfolded proteins.[1b,f]

A wide array of paramagnetic labels are used in protein NMR spectroscopy, including ions bound to native as well as engineered metal-binding sites,[7] chelating tags,[5b] and nitroxide groups,[1e] and a number of protocols have been developed to incorporate the information derived from the use of these labels into structure calculations.[8] One common feature of these methods is that they require additional knowledge about the paramagnetic center, typically in the form of a paramagnetic susceptibility tensor or an electron spin relaxation rate. In this paper we report on the use of a paramagnetic probe that consists of a three-residue *a*mino *t*erminal Cu^{2+}(Ni^{2+})-binding (ATCUN) motif[9] prepended to the N-terminus of a protein via a general, one step recombinant cloning method. We also describe a protocol in which the relaxation-based distance restraints are obtained by treating the electron spin relaxation time as an additional fitting parameter during the course of the structure calculation.

[†] Department of Medical Genetics, University of Toronto.
[#] Department of Biology, York University.
[||] Structural Biology and Biochemistry Program, Hospital for Sick Children.
[‡] Department of Biochemistry, University of Toronto.
[⊥] Protein Engineering Network Centres of Excellence.
[§] Department of Chemistry, University of Toronto.

(1) (a) Wang, P.-L.; Donaire, A.; Zhou, Z. H.; Adams, M. W. W.; La Mar, G. N. *Biochemistry* **1996**, *35*, 11319−11328. (b) Gillespie, J. R.; Shortle, D. *J. Mol. Biol.* **1997**, *268*, 170−184. (c) Bertini, I.; Donaire, A.; Luchinat, C.; Rosato, A. *Proteins: Struct. Func. Genet.* **1997**, *29*, 348−358. (d) Battiste J. L.; Wagner, G. *Biochemistry* **2000**, *39*, 5355−5365. (e) Gaponenko, V.; Howarth, J. W.; Columbus, L.; Gasmi-Seabrook, G.; Yuan, J.; Hubbell, W. L.; Rosevear, P. R. *Protein Sci.* **2000**, *9*, 302−309. (f) Yi, Q.; Scalley-Kim, M. L.; Alm, E. J.; Baker, D. *J. Mol. Biol.* **2000**, *299*, 1341−1351.

(2) (a) Todorovic, S.; Juranic, N.; Macura, S.; Rusnak, F. *J. Am. Chem. Soc.* **1999**, *121*, 10962−10966. (b) Desvaux, H.; Gochin, M. *Mol. Phys.* **1999**, *96*, 1317−1333. (c) Boisbouvier, J.; Gans, P.; Blackledge, M.; Brutscher, B.; Marion, D. *J. Am. Chem. Soc.* **1999**, *121*, 7700−7701.

(3) (a) Banci, L.; Bertini, I.; Bren, K. L.; Cremonini, M. A.; Gray, H. B.; Luchinat, C.; Turano, P. *J. Biol. Inorg. Chem.* **1996**, *1*, 117−126. (b) Allegrozzi, M.; Bertini, I.; Janik, M. B. L.; Lee, Y.-M.; Liu, G.; Luchinat, C. *J. Am. Chem. Soc.* **2000**, *122*, 4154−4161. (c) Shokhirev, N. V.; Walker, F. A. *J. Biol. Inorg. Chem.* **1998**, *3*, 581−594.

(4) Prosser, R. S.; Luchette, P. A.; Westerman, P. W. *Proc. Natl. Acad. Sci. U.S.A.* **2000**, *97*, 9967−9971.

(5) (a) Tolman, J. R.; Flanagan, J. M.; Kennedy, M. A.; Prestegard, J. H. *Proc. Natl. Acad. Sci. U.S.A.* **1995**, *92*, 9279−9283. (b) Gaponenko, V.; Dvoretsky, A.; Walsby, C.; Hoffman, B. M.; Rosevear, P. R. *Biochemistry* **2000**, *39*, 15217−15224.

(6) Ramos, A.; Varani, G. *J. Am. Chem. Soc.* **1998**, *120*, 10992−10993.

(7) (a) Voss, J.; Salwinski, L.; Kaback, H. R.; Hubbell, W. L. *Proc. Natl. Acad. Sci. U.S.A.* **1995**, *92*, 12295−12299. (b) Ma, C.; Opella, S. J. *J. Magn. Reson.* **2000**, *146*, 381−384.

(8) (a) Banci, L.; Bertini, I.; Cremonini, M. A.; Gori-Savellini, G.; Luchinat, C.; Wüthrich, K.; Güntert, P. *J. Biomol. NMR* **1998**, *12*, 553−557. (b) Ubbink, M.; Ejdeback, M.; Karlsson, B. G.; Bendall, D. S. *Structure* **1998**, *6*, 323−335. (c) Tu, K.; Gochin, M. *J. Am. Chem. Soc.* **1999**, *121*, 9276−9285. (d) Hus, J. C.; Marion, D.; Blackledge, M. *J. Mol. Biol.* **2000**, *298*, 927−936.

(9) Harford, C.; Sarkar, B. *Acc. Chem. Res.* **1997**, *30*, 123−130.

10.1021/ja011241p CCC: $20.00
Published on Web 09/15/2001

The ATCUN motif was designed to mimic the Cu^{2+}-binding site of human albumin.[10] This motif, NH_2-X1-X2-His, coordinates a metal via (i) the free N-terminal NH_2 group from residue X1, (ii) two backbone amide groups from residues X2 and His, and (iii) the imidazole group of a His residue.[10] The site has a high binding affinity for paramagnetic Cu^{2+}, which is coordinated by the four nitrogens in a distorted square-planar geometry. In this configuration, the energy gap between the ground and excited states of copper ($S = {}^1/_2$) is substantial, resulting in relatively long electronic relaxation times (τ_e) on the order of nanoseconds,[11] and only small anisotropy of the **g**-tensor.[12] In turn, this leads to efficient relaxation of the nuclear spins via dipolar interaction with the copper ion and to near-absence of pseudocontact chemical shifts.

Results and Discussion

Human ubiquitin was chosen as a model system to investigate the utility of the Cu^{2+}-ATCUN motif as a paramagnetic probe for deriving long-range distance restraints in proteins. Cloning, expression, and purification of ATCUN-ubiquitin were carried out according to a straightforward protocol described in the Materials and Methods section. The three-residue ATCUN motif (Gly-Ser-His in this case) was followed by a single glycine residue linker to minimize potential structural perturbations to ubiquitin. Note that in many cases prepending an ATCUN tag to a protein is more straightforward than the addition of spin-labeling reagents that react at the free thiol of cysteine since several rounds of site-directed mutagenesis and activity assays may be necessary to ensure that only one solvent-accessible cysteine is available for derivatization and that the protein structure is not perturbed.

NMR spectra (500 MHz ^{1}H frequency) were collected at 30 °C on matched 0.6 mM uniformly ^{15}N-labeled samples of metal-free and paramagnetic Cu^{2+}-loaded protein. Chemical shifts in ATCUN-ubiquitin were found to be similar to those in the native protein with the exception of several terminal residues; a small number of ambiguities were resolved by verifying the backbone assignment using an HNCACB experiment[13] recorded on a uniformly labeled ^{15}N,^{13}C sample. Transverse relaxation rates of the amide protons, R_2^{HN}, were measured using the HSQC-based pulse sequence shown in Figure 1. The relaxation rates, R_2^{HN}, were found to be independent of protein concentration as confirmed by an additional series of measurements on a 0.3 mM sample. Representative relaxation profiles fit by a single-exponential decay curve are shown in Figure 2.

The paramagnetic relaxation enhancements, $\Gamma_2^{HN} = R_2^{HN}(Cu^{2+}) - R_2^{HN}(\text{free})$, were interpreted by using the Solomon−Bloembergen equation:[14]

$$\Gamma_2^{HN} = \frac{1}{r_{HN-Cu}^6}\left\{\frac{1}{15}\left(\frac{\mu_0}{4\pi}\right)^2 \hbar^2 \gamma_H^2 g_{Cu}^2 \beta^2 S(S+1)\left(4\tau_c + \frac{3\tau_c}{1+\omega_H^2\tau_c^2}\right)\right\} \quad (1)$$

where the electronic g factor has been determined by ESR measurements,[12] $g_{Cu} = 2.09$, and the correlation time τ_c reflects the combined effect of molecular tumbling and electron spin relaxation, $1/\tau_c = 1/\tau_r + 1/\tau_e$. The rotational correlation time, τ_r, was determined in this study by using ^{15}N T_1 and T_2 data yielding 3.4 ns at 30 °C with the rotational diffusion tensor very close to isotropic $D_\parallel/D_\perp \cong 1.0$ in both metal-free and Cu^{2+}-loaded forms.[15] It is noteworthy that the Curie spin contribution to proton relaxation is negligible in this case and that the point-dipole approximation implied by eq 1 appears to hold well for protons relaxed via dipolar interaction with the Cu^{2+} electron

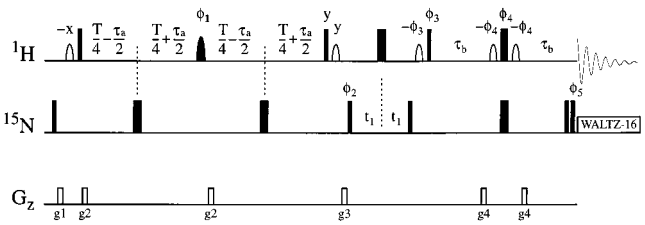

Figure 1. Pulse scheme used to measure T_2 paramagnetic relaxation rate enhancements of amide protons in ^{15}N-labeled proteins. All narrow (wide) pulses are applied with a flip angle of 90° (180°) along the x-axis unless indicated otherwise. The rectangular ^{1}H (^{15}N) pulses are applied with a field of 35 kHz (6.5 kHz) and are centered at 4.77 ppm (119 ppm). Open shaped pulses represent 1.6 ms water-selective pulses applied with a rectangular profile. The filled shaped pulse corresponds to a 2.50 ms REBURP pulse[28a] applied at 8.54 ppm with a field strength of 2.50 kHz to selectively excite ^{1}HN and not ^{1}Hα resonances. ^{15}N decoupling is achieved by using a WALTZ-16 sequence[28b] with a 1 kHz field. The delays used are $\tau_a = 2.75$ ms ($= 1/(4J_{HN})$) and $\tau_b = 2.30$ ms. Ten delays, T, in the range from 6.5 to 65.0 ms have been used to sample the relaxation decay with an additional series of measurements for rapidly relaxing peaks employing delays in the range from 6.5 to 14.5 ms. The phase cycle is the following: $\phi_1 = 2(x)$, $2(y)$, $\phi_2 = 4(x)$, $4(-x)$, $\phi_3 = (x, -x)$, $\phi_4 = 2(x)$, $2(-x)$, $\phi_5 = (x, -x)$, rec $= (x, 2(-x), x, -x, 2(x), -x)$. Quadrature detection in F_1 is accomplished by States-TPPI incrementation of ϕ_2.[28c] The durations and strengths of the gradients are the following: g1 = (1.0 ms, 5 G/cm), g2 = (0.1 ms, 12 G/cm), g3 = (1.0 ms, 15 G/cm), g4 = (0.4 ms, 25 G/cm).

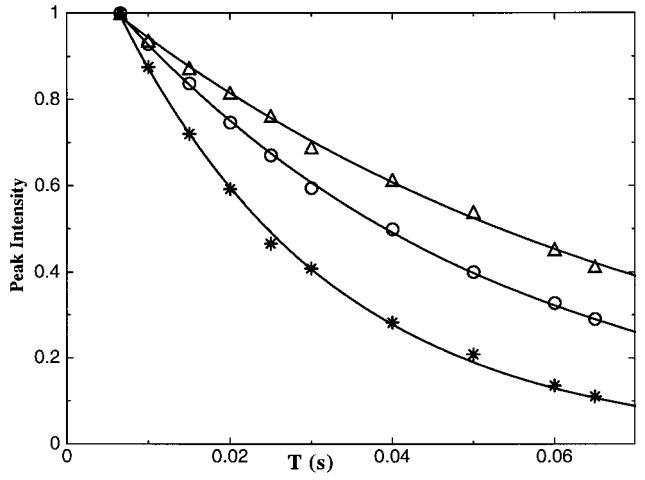

Figure 2. T_2 relaxation decay profiles of three representative amide protons in Cu^{2+}-loaded ATCUN-ubiquitin. Peak intensities were fit with a single exponential yielding relaxation decay times of 47.3 (Asn 25, ○), 68.3 (Arg 54, △), and 26.2 ms (Ser 65, ∗).

(10) Lau, S.; Kruck, T. P. A.; Sarkar, B *J. Biol. Chem.* **1974**, *249*, 5878−5884.

(11) Banci, L.; Bertini, I.; Luchinat, C. *Nuclear and Electron Relaxation*; VCH: Weinheim, Germany, 1991.

(12) Rakhit, G.; Antholine, W. E.; Froncisz, W.; Hyde, J. S.; Pilbrow, J. R.; Sinclair, G. R.; Sarkar, B. *J. Inorg. Biochem.* **1985**, *25*, 217−224.

(13) (a) Wittekind, M.; Mueller, L. *J. Magn. Reson.* **1993**, *B101*, 201−205. (b) Muhandiram, D. R.; Kay, L. E. *J. Magn. Reson.* **1994**, *B103*, 203-216.

(14) Solomon, I.; Bloembergen, N. *J. Chem. Phys.* **1956**, *25*, 261−266.

(15) (a) Lee, L. K.; Rance, M.; Chazin, W. J.; Palmer, A. G. *J. Biomol. NMR* **1997**, *9*, 287−298. (b) Farrow, N. A.; Muhandiram, R.; Singer, A. U.; Pascal, S. M.; Kay, C. M.; Gish, G.; Shoelson, S. E.; Pawson, T.; Forman-Kay, J. D.; Kay, L. E. *Biochemistry* **1994**, *33*, 5984−6003. (c) Tjandra, N.; Feller, S. E.; Pastor, R. W.; Bax A. *J. Am. Chem. Soc.* **1995**, *117*, 12562−12566. (d) Lee, A. L.; Wand, A. J. *J. Biomol. NMR* **1993**, *13*, 101−112.

spin.[16] However, there is a possibility that local ATCUN dynamics may modulate the r_{HN-Cu} distance, resulting in an additional relaxation contribution unaccounted for by eq 1.

Γ_2^{HN} values were analyzed with use of a new module, PMAG, written in-house for the program CNS.[17] The pseudopotential E_{pmag} incorporated in the target function of CNS is defined as:

$$E_{pmag} = k_{pmag}\sum(\Gamma_2^{calc} - \Gamma_2^{obs})^2\left[1 - \exp\left\{-\left(\frac{\Gamma_2^{calc} - \Gamma_2^{obs}}{\sqrt{2}\sigma_\Gamma^{obs}}\right)^2\right\}\right] \quad (2)$$

where Γ_2^{obs} is the experimentally observed paramagnetic relaxation rate enhancement, Γ_2^{calc} is the relaxation enhancement calculated from eq 1 by using the distance r_{HN-Cu}^{calc} obtained at a given time in the simulated annealing protocol, and σ_Γ^{obs} is the uncertainty in Γ_2^{obs} estimated from the experimental data. The summation over all residues for which the relaxation data are available is implied. During each CNS iteration eq 2 is evaluated by using a set of different correlation times, τ_c, extending over a preselected range from τ_c^{low} to τ_c^{high} and the lowest E_{pmag} value is returned to the program. Thus, τ_c is essentially optimized "on the fly" during the course of the structure calculations. Note that the multiplicative factor in square brackets in eq 2 accounts for the experimental uncertainty so that the penalty is reduced if the difference between Γ_2^{calc} and Γ_2^{obs} falls within the bounds of the experimental error. Finally, since the potential of eq 2 rises steeply with a decrease in r_{HN-Cu}^{calc} we have also implemented a parabolic "soft asymptote"[17] for this function to avoid unreasonably high E_{pmag} contributions (see Supporting Information).

The observed paramagnetic relaxation rates were interpreted in conjunction with the X-ray structure of ubiquitin.[18] The coordinates of the ATCUN motif[19] were added to the X-ray coordinate set and the resulting structure was refined as described in the Materials and Methods section. Figure 3 shows the 10 lowest energy conformations out of 100 calculated, with the protein backbone structures superimposed. The coordinates of the Cu atom (shown as spheres in the plot) are determined with a root-mean-square deviation (rmsd) of 0.5 Å (based on superposition of the backbone atoms of ubiquitin) and the correlation time, τ_c, obtained from this procedure is 1.5 ± 0.6 ns, which corresponds to an electron relaxation time, τ_e, of 2.7 ± 0.3 ns. Using a Monte Carlo approach, we have established that the uncertainty in the position of the copper and the related significant uncertainty in the determined correlation time τ_c can be largely attributed to measurement error (σ_Γ^{obs}). It is worth noting that the spatial distribution of the copper atoms in Figure 3 reflects a "valley" on the potential energy surface where the paramagnetic restraints are satisfied almost equally well within the current level of the experimental uncertainty. The inset in Figure 3 shows the structure of the ATCUN motif (Gly-Ser-His) and the linker (Gly) from the lowest energy conformation of ATCUN-ubiquitin generated in this series of calculations.

It is noteworthy that the HSQC correlations for residues 16−18 and 20−21 (residue 19 is a proline) in the spectrum of Cu^{2+}-loaded ATCUN-ubiquitin have been broadened beyond detection, which is consistent with the calculated structure. This result is significant since the disappearance of peaks upon addition of Cu^{2+} has not been used as a source of constraints in structure calculations. The agreement between the observed and calculated paramagnetic relaxation rates is illustrated in Figure 4a for the lowest energy structure and the corresponding correlation between the distances is shown in Figure 4b.

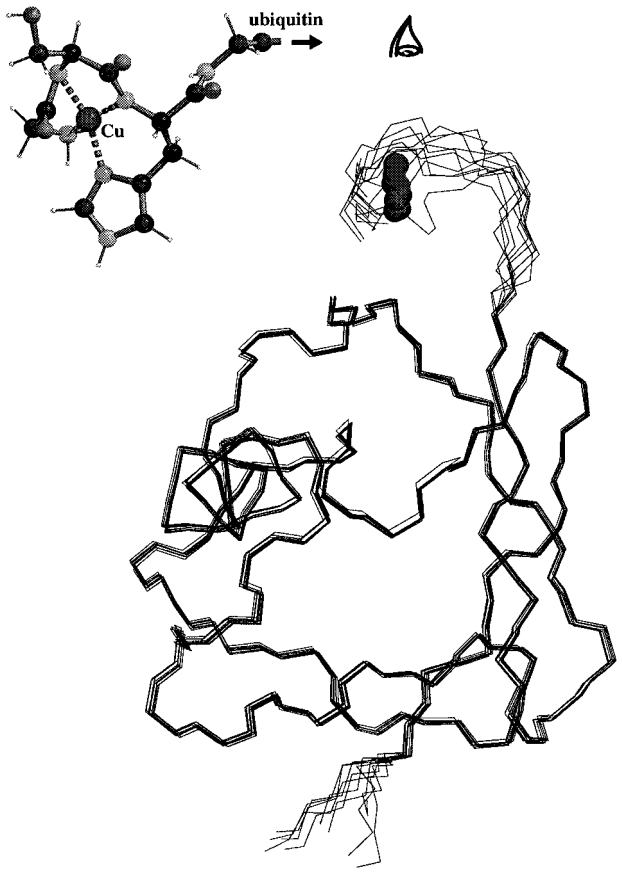

Figure 3. The 10 lowest energy structures of ATCUN-ubiquitin calculated with the pseudopotential E_{pmag}, eq 2, comprising 50 experimental paramagnetic restraints. During low-temperature simulated annealing the backbone dihedral angles of ubiquitin (residues 3 to 69) were fixed according to their X-ray crystallographic values,[18] whereas all other backbone and side-chain torsional angles were optimized. The resulting structures were subsequently refined by using a conjugate gradient minimization. The spheres in the plot represent Cu^{2+} ions. The backbone conformation of the calculated structures is nearly identical to that of the crystal structure with an average rmsd of 0.14 Å for the heavy backbone atoms from residues 3−69. The inset shows the N-terminal residues of ATCUN-ubiquitin (Gly-Ser-His comprising the metal-binding motif, followed by a Gly linker) from the lowest energy ATCUN-ubiquitin structure (view from above as indicated in the plot).

Because of its small size, the ATCUN motif is likely to introduce minimum perturbations to either structure or function when tagged to most proteins. We suggest that the ATCUN tag will be useful for high-precision structure determination when used in conjunction with other paramagnetic labels. The success of recent structural studies using multiple paramagnetic labels has been well-documented[1e,20] and such studies are expected to further benefit from the increased diversity of available labels. Furthermore, the ATCUN motif can be used as an efficient low-resolution structural probe of protein

(16) Ma, L. X.; Jorgensen, A. M. M.; Sorensen, G. O.; Ulstrup, J.; Led, J. J. *J. Am. Chem. Soc.* **2000**, *122*, 9473−9485.

(17) Brünger, A. T.; Adams, P. D.; Clore, G. M.; Delano, W. L.; Gros, P.; Grosse-Kunstleve, R. W.; Jiang, J. S.; Kuszewski, J.; Nilges, M.; Pannu, N. S.; Read, R. J.; Rice, L. M.; Simonson, T.; Warren, G. L. *Acta Crystallogr.* **1998**, *D54*, 905−921.

(18) Alexeev, D.; Bury, S. M.; Turner, M. A.; Ogunjobi, O. M.; Muir, T. W.; Ramage, R.; Sawyer, L. *Biochem. J.* **1994**, *299*, 159−163.

(19) Camerman, N.; Camerman, A.; Sarkar, B. *Can. J. Chem.* **1976**, *54*, 1309−1316.

(20) Aronoff-Spencer, E.; Burns, C. S.; Avdievich, N. I.; Gerfen, G. J.; Peisach, J.; Antholine, W. E.; Ball, H. L.; Cohen, F. E.; Prusiner, S. B.; Millhauser, G. L. *Biochemistry* **2000**, *39*, 13760−13761.

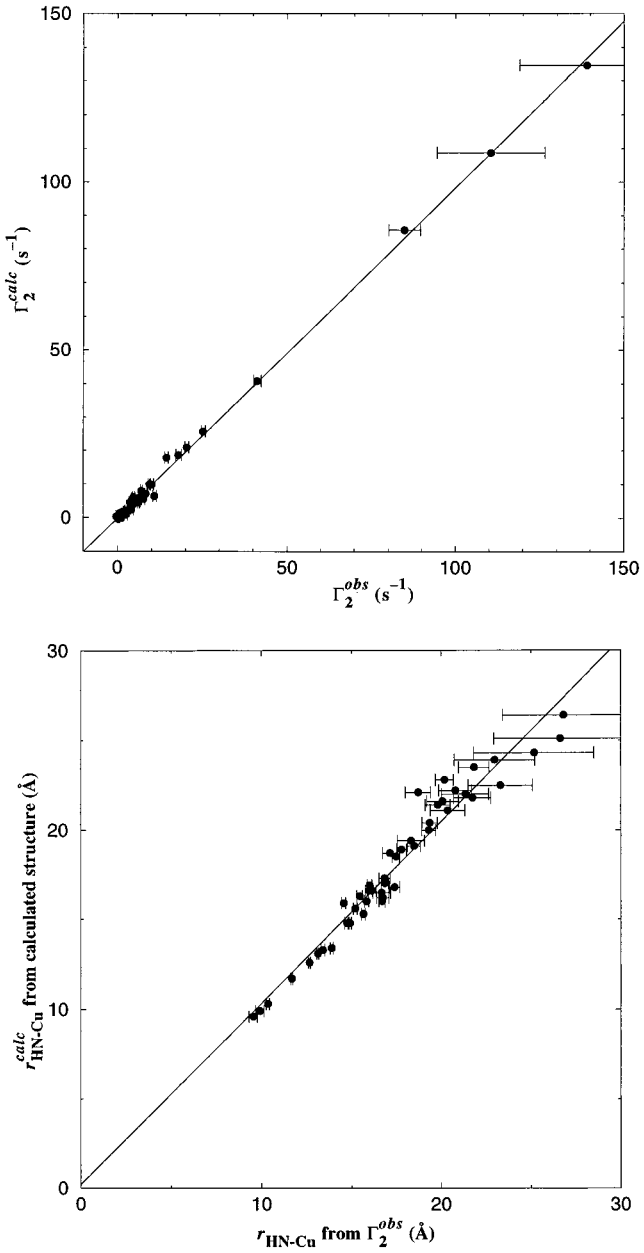

Figure 4. (a) Correlation between the measured paramagnetic relaxation rate enhancements Γ_2^{obs} and the corresponding enhancements Γ_2^{calc} calculated from eq 1 by using the lowest energy ATCUN-ubiquitin structure (see Figure 3) together with the optimized value of τ_c. (b) Correlation between the ^{1}HN−Cu distances extracted from Γ_2^{obs} data using eq 1 and the corresponding distances in the lowest energy ATCUN-ubiquitin structure.

complexes and multidomain proteins. Using ubiquitin as an example, the method presented here can be employed to study multi-ubiquitin chains[21] and interactions with ubiquitin-conjugating enzymes.[22] Determination of ligand binding sites and characterization of disordered states of proteins are other applications for which the ATCUN motif is anticipated to be useful.

Materials and Methods

Cloning, Expression, and Purification of ATCUN-Ubiquitin. A DNA fragment encoding the ATCUN motif, Gly-Ser-His, a single residue glycine linker, and residues 1−72 of ubiquitin was PCR amplified and ligated into the vector pGEX-4T2 (Pharmacia) at BamHI and EcoRI restriction sites. The linker (which can be of variable length) is added to ensure that the protein structure is relatively unperturbed. In general, the choice of linker length is based on a compromise: a long linker is less likely to perturb the protein but, on the negative side, can contribute significantly to the mobility of the paramagnetic tag. Isotopically ^{15}N-labeled [glutathione *S*-transferase]-ATCUN-ubiquitin fusion protein was obtained by affinity purification of a soluble extract of *E. coli* BL21::DE3 (Novagen) cells grown in minimal media supplemented with 1 g/L (^{15}N,99%)-ammonium chloride. ATCUN-ubiquitin was liberated from the fusion protein by treatment with human thrombin (Sigma) and subsequently purified to homogeneity by gel filtration. Though ATCUN-ubiquitin could have been cloned and produced directly, we favor the fusion protein method as a general approach. Proteins produced in *E. coli* as GST fusions tend to be soluble and well expressed. In addition, the insertion of gene fragments into the BamHI site followed by thrombin protease cleavage guarantees a protein that begins with Gly-Ser, the first two residues of the ATCUN motif, with a free N-terminal amino group for coordination with paramagnetic Cu^{2+}. Otherwise, direct overexpression of the protein may lead to the presence of N-terminal Met or loss of N-terminal residues due to misprocessing by endogenous bacterial aminopeptidases.[23]

Coordination of copper was achieved by the addition of 1.1 molar equiv. of $CuSO_4$ to a 20 μM protein solution previously dialyzed in water at pH 4.5. After the pH was raised to 6.8, 5 μL of Chelex-100 beads (BioRad) were added to the protein solution to remove excess metal. As $Cu(OH)_2$ is insoluble, it may also be possible to remove free metal by increasing the pH above neutral. Concentrated Cu^{2+} loaded samples had a characteristic pink-purple hue with a broad absorption maximum centered at 525 nm ($\epsilon = 100-150$ M^{-1} cm^{-1}). The affinity of Cu^{2+} for the ATCUN moiety is very high with a dissociation constant of 2×10^{-17} measured for an isolated ATCUN motif.[24]

NMR Data Collection. All NMR data were acquired on a 500 MHz Varian Unity Inova spectrometer equipped with a pulsed-field gradient accessory. All spectra were processed with nmrPipe software[25a] and interpreted with the software packages nmrDraw,[25a] NMRView,[25b] and PIPP.[25c] Peak intensities were fitted by using the nonlinear least-squares fitting algorithm nlinLS, part of the nmrPipe software package. Exponential fitting of the decay curves was accomplished by using in-house software that was originally described by Farrow et al.[15b] The errors σ_Γ^{obs} were obtained from the fitting of the decay curves using a standard Monte Carlo approach.[15b]

Additional measurements performed on an ATCUN-ubiquitin sample loaded with diamagnetic Ni^{2+} revealed the presence of two slowly exchanging species representing free and metal-bound forms as observed previously.[26] In contrast, metal-free and Cu^{2+}-bound forms produced a single set of resonances. The relaxation rates R_2^{HN} measured in the Cu^{2+}-containing samples with high protein concentrations (around 2 mM) showed a significant concentration dependence for several residues. This effect, likely attributable to intermolecular paramagnetic relaxation, was negligible at lower protein concentrations as confirmed by the data from 0.6 and 0.3 mM samples.

CNS Structure Calculations. A set of atomic coordinates representing the X-ray structure of ubiquitin (protein database accession code 1UBI[18]) with a prepended ATCUN motif[19] was prepared. In what follows residue numbering in ubiquitin has been preserved, while the residues Gly-Ser-His from the ATCUN motif and the Gly linker were assigned numbers from −3 to 0. The structure was equilibrated by using a standard CNS protocol with the coordinates of the atoms from residues 3 to 69 of ubiquitin fixed. Subsequently, the structure was refined

(21) Phillips, C. L.; Thrower, J.; Pickart, C. M.; Hill, C. P. *Acta Crystallogr.* **2001**, *D57*, 341−344.

(22) Huang, L.; Kinnucan, E.; Wang, G. L.; Beaudenon, S.; Howley, P. M.; Huibregtse, J. M.; Pavletich, N. P. *Science* **1999**, *286*, 1321−1326.

(23) Hirel, P.-H.; Schmitter, J.-M.; Dessen, P.; Fayat, G.; Blanquet, S. *Proc. Natl. Acad. Sci. U.S.A.* **1989**, *86*, 8247−8251.

(24) Kruck, T. P. A.; Lau, S.; Sarkar, B. *Can. J. Chem.* **1976**, *54*, 1300−1308.

(25) (a) Delaglio, F.; Grzesiek, S.; Vuister, G. W.; Zhu, G.; Pfeifer, J.; Bax, A. *J. Biomol. NMR* **1995**, *6*, 277−293. (b) Johnson, B. A.; Blevins, R. A. *J. Biomol. NMR* **1994**, *4*, 603−614. (c) Garrett, D. S.; Powers, R.; Gronenborn, A. M.; Clore, G. M. *J. Magn. Reson.* **1991**, *95*, 214−220.

(26) Gasmi, G.; Singer, A.; Forman-Kay, J. D.; Sarkar, B. *J. Peptide Res.* **1997**, *49*, 500−509.

against the set of experimental restraints Γ_2^{obs} by using the pseudopotential described in the text, eq 2, implemented in the module PMAG. The refinement consisted of 40 rounds of torsion angle dynamics[27] as the system was cooled from 2000 to 0 K with each round consisting of 10 ps of molecular dynamics (1 fs time step). Backbone dihedral angles of residues 3 to 69 of ubiquitin were fixed while all other backbone and side-chain dihedral angles were allowed to vary. Following this step, the structure was subjected to Powell conjugate-gradient minimization in the presence of the Γ_2^{obs} restraints. Note that the aim of this procedure is to determine the relative position of the protein and the ATCUN motif, with the backbone structure of ubiquitin remaining essentially preserved.

During the torsion angle dynamics stage the van der Waals interaction force constant was ramped from 0.1 to 1.0 kcal/Å^2. The force constant k_{pmag} (eq 2) was ramped from 0.1 to 2.0 kcal·s^2 and maintained at 2.0 kcal·s^2 during the subsequent conjugate-gradient minimization. At each iteration in the CNS computations E_{pmag} is calculated for a number of τ_c values and the lowest obtained value is returned to the program. In this application, τ_c is varied between $\tau_c^{low} = 0.1$ ns and $\tau_c^{high} = 4.0$ ns with a step size of 0.1 ns. The parabolic extension for the pseudopotential E_{pmag} has been implemented, to avoid unreasonably high E_{pmag} energies, as follows. When the E_{pmag} term calculated for an individual residue i using eq 2 exceeds a user-defined threshold (in this application 3000 kcal) this contribution is automatically recalculated according to the formula $c_1^i(r_{HN-Cu}^{calc} - c_2^i)^2$. The numeric coefficients c_1^i and c_2^i in this expression are determined in the PMAG module for each residue i to ensure the continuity of the pseudopotential function and its first derivative with respect to r_{HN-Cu} at the threshold level. The threshold should be lowered if high-temperature molecular dynamics is employed to avoid an excessive buildup of energy. It is worth pointing out that, for a given set of atomic coordinates, E_{pmag} shows a pronounced minimum as a function of τ_c (see Supporting Information).

The results of the CNS-based data analysis were verified by using a simple minimization procedure implemented with Matlab software (MathWorks Inc.). In this alternative approach the paramagnetic penalty function, eq 2, was minimized by direct fitting of τ_c and $\{x, y, z\}_{Cu}$ (three coordinates of the paramagnetic center in the coordinate frame of the X-ray structure). Note that any steric constraints for ATCUN placement are ignored in this simplified approach. The results are in agreement with the CNS procedure and the quality of the correlation between the experimental and calculated rate constants is very good.

Acknowledgment. N.R.S. is the recipient of a Centennial Fellowship from the Canadian Institutes of Health Research (CIHR). Funding from CIHR and AstraZeneca is gratefully acknowledged. L.E.K. is an international investigator of the Howard Hughes Medical Research Institute.

Supporting Information Available: Two figures illustrating the dependence of E_{pmag} on r_{HN-Cu} and on τ_c (PDF). This material is available free of charge via the Internet at http://pubs.acs.org. The modified CNS software package which includes the PMAG module is available at http://pound.med.utoronto.ca/atcun.

JA011241P

(27) Stein, E. G.; Rice, L. M.; Brünger, A. T. *J. Magn. Reson.* **1997**, *124*, 154−164.

(28) (a) Geen, H.; Freeman, R. *J. Magn. Reson.* **1991**, *93*, 93−141. (b) Shaka, A. J.; Keeler, J.; Frenkiel, T.; Freeman, R. *J. Magn. Reson.* **1983**, *52*, 335−338. (c) Marion, D.; Ikura, M.; Tschudin, R.; Bax, A. *J. Magn. Reson.* **1989**, *85*, 393−399.